Renormalization of miscible flow functions

1990 J. Phys. A: Math. Gen. 23 4199

(http://iopscience.iop.org/0305-4470/23/19/009)

J. Phys. A: Math. Gen. **23** (1990) 4199-4209. Printed in the UK

Renormalization of miscible flow functions

M I Morris and R C Ball

Cavendish Laboratory, Madingley Road, Cambridge, UK

Received 30 January 1990

Abstract. We present a numerical renormalization study of two-phase, viscous fingering flow in a uniform two-dimensional porous medium. Iterating our procedure gives the effective flow parametrization appropriate to successively larger scales and enables us to compute flow functions that can be used to simulate kilometre-sized oil reservoirs, starting from functions appropriate to 10 cm core samples. We parametrize the local flow in terms of the fractional and total flows across a block as functions of the average composition and pressure gradient across the block. From numerical simulations on a fine grid, we measure the corresponding flow functions for larger blocks: these show only limited statistical scatter and so allow us to define a renormalization. We discuss the range of physically significant fractional flow and total mobility functions, and find evidence for non-trivial fixed point behaviour of these functions in the fingering instability regime.

1. Introduction

It is well known that when a less viscous fluid displaces a more viscous one through a porous medium, application of Darcy's law to each fluid gives rise to the unstable growth of interface corrugations into a highly fingered flow (see Scheidegger 1971, for example). Capillary pressures, differential wetting, diffusional and dispersive mixing can all mitigate the instability, but there are important processes, such as secondary oil recovery, for which the suppression is of only limited effect.

The conventional approach to such 'two-phase flow' is via a phenomenological description appropriate to a single, truly mixed phase of two components; the fluxes of each phase are then given uniquely in terms of the gradients of macroscopic averages—in particular pressure and composition. Because on the large scale the two phases are interdigitated (in a manner determined by the preceding flow history) rather than mixed, there can be no exact description of the flow properties of the effective mixture which is not statistical. Nevertheless, we might hope to find a single dominant large-scale behaviour from the ensemble of possible interdigitation patterns generated by the flow process.

In this paper we explicitly test the assumption that a large-scale parametrization is possible and show that the scatter in the behaviour observed is modest in comparison with the overall clear trend. We focus on the most extreme case with fewest parameters, namely two-fluid displacement in a homogeneous medium with adverse viscosity ratio only. Thus our fluids are 'miscible' in the sense that they have no mutual surface tension or preferential wetting, but we do not incorporate any explicit local mixing effects.

0305-4470/90/194199+11$03.50

Without the assumption of molecular mixing we adopt the following formulation for the fluxes of each component:

$$q_1(c) = -\lambda(c) f(c) \nabla p$$

$$q_2(c) = -\lambda(c)(1 - f(c)) \nabla p$$

where $c \equiv c_1$ is the composition fraction of component 1, and we choose units such that $c_2 = 1 - c$. Thus $\lambda(c)$ is the total mobility governing the total flux

$$q = 1_1 + q_2 = -\lambda(c) \nabla p$$

and $f(c)$ is the fractional flow of component 1,

$$q_1 = f(c) q.$$

For the case of a truly mixed phase, the fractional flow would become simply $f(c) = c$. We assume incompressibility,

$$\nabla \cdot q = 0$$

and track the evolution of composition through

$$\frac{\partial c}{\partial t} + \nabla \cdot q_1 = 0.$$

Our results are cast in the form of a renormalization—the flow properties of a super-cell that represent the observed relation between the appropriately averaged flow properties of its constituent single cells. The success of the procedure is explicitly tested in two ways. Firstly, we find that the numerical scatter in the renormalized flow properties over different realizations is not large enough to prevent useful comparison between these and the input, single cell properties. Secondly, we confirm that the iteration of two small scale renormalizations gives results equivalent to those from the corresponding (but computationally more costly) single-step large-scale renormalization.

2. Numerical simulation

All the work reported here is based on a solution of the above flow equations in a two-dimensional line drive geometry by a fine grid simulation code developed by BP. The basic algorithm uses Peaceman's total velocity formulation in an explicit finite difference form based on flux corrected transport, to minimize numerical dispersion problems that arise from sharp concentration gradients. It has been tested extensively against experimental data, with favourable results (Christie and Bond 1987, Christie 1988). We have performed the displacement under the constraint that the rate of injection of the displacing fluid is held constant, and for all the results reported here we have triggered the fingering instability by placing random initial concentrations at the injection end of the drive, with viscosity ratio $\mu_2/\mu_1 = 10$.

3. Renormalized flow functions

We begin by performing a simulation on a given grid (of $l \times w$ blocks) using core sample data, for example, to prescribe the fractional flow and total mobility functions

for each block. From the results of this simulation, flow functions appropriate to a renormalization cell of size m × m grid blocks are computed. These new functions are used in a further simulation from which another pair of renormalized flow functions is similarly computed. In principle such a scheme can be iterated as many times as necessary to find flow functions that will facilitate the use of only a moderate number of grid blocks to describe a physically large flow, thereby providing a practicable method of relating core scale flow data to reservoir scale behaviour.

The flow functions appropriate to a renormalization cell are calculated using the grid block pressure and concentration fields obtained from the numerical simulation results. For the fractional flow and total mobility respectively, the renormalized functions are,

$$\tilde{f}(\tilde{c}) = \sum_{i,j} f(c_{ij})\lambda(c_{ij})\nabla p_{ij}\left(\sum_{i,j} \lambda(c_{ij})\nabla p_{ij}\right)^{-1}$$

and

$$\tilde{\lambda}(\tilde{c}) = \sum_{i,j} \lambda(c_{ij})\nabla p_{ij}\left(\sum_{i,j} \nabla p_{ij}\right)^{-1}$$

with renormalized concentration given by

$$\tilde{c} = \sum_{i,j} c_{ij}\left(\sum_{i,j} 1\right)^{-1}$$

where the sums are over grid blocks within the renormalization cell. In the above equations, only the drive direction components of the flux and pressure gradient have been used for this study. By performing these calculations using concentration and pressure data from various times during the displacement, the functional dependence on (renormalized) concentration is obtained.

We next consider the physical basis for choosing functional forms for f and λ. Given that the domain of flow behaviour presented by our flow equations excludes rate-dependent terms, there are two limiting cases of fluid flow, namely series flow of the two components, and flow in parallel. These flow configurations give respectively the minimum and maximum values of both total flux and fractional flow for a given concentration and pressure drop across a grid block. (In other physical systems there may be configurations that extend beyond these limits, turbulence, for example, would give a lower total flux than series flow.) The series flow functions are

$$f_s(c) = c$$

$$\lambda_s(c) = \frac{1}{c\mu_1 + (1-c)\mu_2}$$

and those for parallel flow are

$$f_p(c) = \frac{c}{(c + (1-c)(\mu_1/\mu_2))}$$

$$\lambda_p(c) = \frac{c}{\mu_1} + \frac{1-c}{\mu_2}.$$

Experimentally, it has been found that for well mixed fluids, the viscosity of the mixture is well represented by a 'quarter power mixing rule' (Koval 1963), that is

$$\lambda(c)=\left(\frac{c}{\mu_1^n}+\frac{1-c}{\mu_2^n}\right)^{1/n} \tag{1}$$

with $n=0.25$. The general form of equation (1) encompasses the series ($n=-1$) and parallel ($n=+1$) flow cases discussed above, and we adopt it in numerical fitting below. In the light of remarks made above, only values of n in the range $|n|\leqslant 1$ have physical significance.

Given the forms of f_s and f_p, and by analogy with the total mobility, we have chosen the following one-dimensional parametrization for fractional flow:

$$f(c)=\frac{c}{c+(1-c)(\mu_1/\mu_2)^{1-\omega}}. \tag{2}$$

This form is also that given by the Todd and Longstaff (1972) parametrization for their notion of effective viscosity. The functions f_s and f_p correspond to $\omega=1$ and $\omega=0$ respectively, and the range of physical validity is $0\leqslant\omega\leqslant 1$.

In general it is to be expected that projecting the two function space ($f(c)$, $\lambda(c)$) onto a two-dimensional plane (in our case the n-ω plane defined by (1) and (2)) represents a severe approximation. However our particular choice incorporates the bounds discussed above, and generally fits most of our data within the limitations of the latter. We have found that, although there is sometimes a small amount of motion out of the n-ω plane (as gauged by the quality of fit), working in this plane does discover physically meaningful behaviour.

4. Boundary effects

The renormalization scheme described above is meaningful only if the renormalization cell is of a size and position in the flow such that effects due to the boundaries of the grid are not incorporated into the renormalized flow functions. This is an important constraint, and validating criteria for the positioning of the renormalization cell are presented here.

From our simulation results we have found that the fingering formation is largely determined roughly by the time it has reached the position down the drive equal to the drive width. Thereafter, the transverse development of the fingers is substantially limited by the presence of the side boundaries, which are reflecting walls in our case—the use of periodic boundaries might reduce this effect, but we have not so far investigated this possibility. Accounting for the grid end boundaries is also important, because as some particular finger approaches breakthrough, the entire flow can be strongly perturbed. For flow functions that tend to suppress fingering, the displacement can become very diffuse with the consequence that breakthrough may occur before the renormalized concentration becomes very high, although to some extent this effect is offset by the fact that breakthrough less strongly perturbs the whole drive for such diffuse displacements. In general, obtaining the concentration dependence of the renormalized flow functions to a satisfactory extent requires that the drive must be sufficiently long.

The maturing of the fingers by the time they are a distance down the drive equal to the drive width relates significantly to the issue of where to place the renormalization cell. If it is placed too far down the drive, production end and side boundary effects will be included. If it is placed too near the injection end, the fingering will not be well developed and this will bias the renormalized flow functions towards those applying at the grid block level.

In all the cases we have considered, we have used a grid of aspect ratio three to account for the problems associated with breakthrough whilst seeking to avoid the use of very many-grid blocks. Given this regime, it is the ratio of the drive width to the size of the renormalization cell, w/m, that determines the influence of the boundaries on the renormalized flow functions. Plainly the larger the ratio the more confident we can be that the associated flow functions will be independent of boundary effects. But this has to be related to the penalties associated with either large w (requiring very many grid blocks) or small m (increasing the number of renormalization iterations—and hence the degree of approximation—required to model large-scale flows).

We have found that with our grid of aspect ratio three, a value of six for the ratio w/m satisfactorily suppresses the boundary effects, which allows for a renormalization cell of size 6×6 with the grid of size 108×36 grid blocks that we have mostly been using. For this grid, we have placed the renormalization cell at grid blocks 22-27 inclusive in the drive direction. This size of renormalization cell would allow us to simulate reservoirs of kilometre size with only three or four renormalizations from the core scale.

To show the effect of the ratio w/m, consider the renormalized flow functions appropriate to a 6×6 cell computed from simulation results for three different grids, 36×12, 108×36 and 216×72, with the cell being in the equivalent positions 6-11, 22-27 and 47-52 respectively in the drive direction. Such data are shown in figure 1 for which the grid block flow functions correspond to the point (0.25, 1.0) in the n-ω plane. The scatter in the fractional flow data from the two larger grids makes it difficult to say more than that they are broadly in agreement, and that the small grid data lie

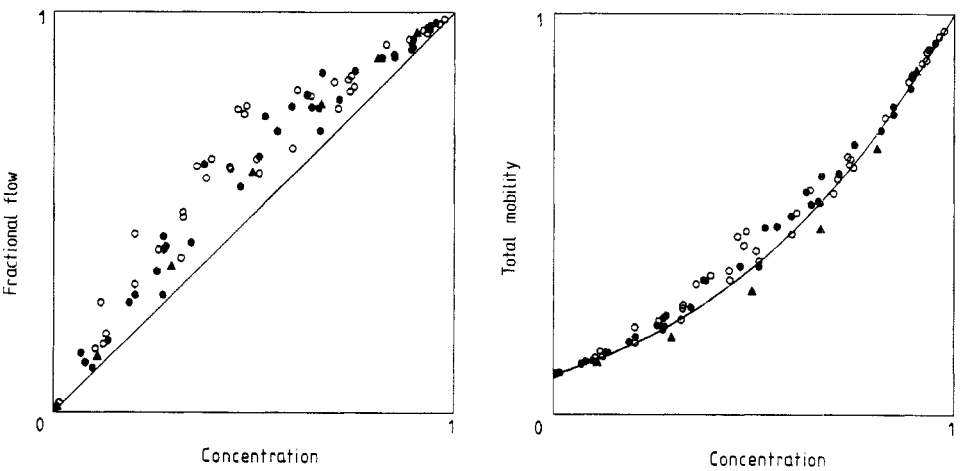

Figure 1. Comparison of fractional flow (*a*) and total mobility (*b*) data for [6×6] renormalization of perfect mixing with a quarter-power viscosity mixing rule, for three different values of w/m: filled triangles, $w/m=2$; open circles, $w/m=6$; filled circles, $w/m=12$. The curves are the initial grid block functions.

towards the lower boundary of the envelopes of the larger grid data. The total mobility data are more conclusive. Whilst the data from the larger grids are in good agreement within the scatter, being roughly bounded below by the quarter power rule, that from the smaller grid is significantly lower than this rule at intermediate concentrations. On the basis of this and other simulations we find that this dipping down of the total

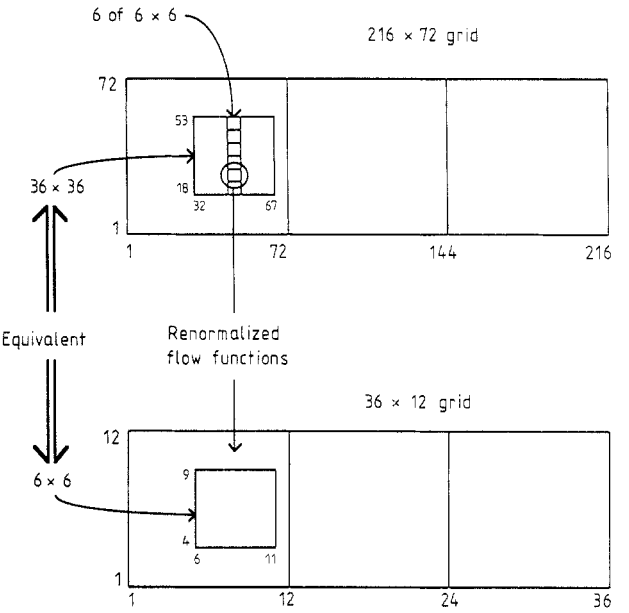

Figure 2. Schematic of consistency test applied to the renormalization procedure. Data from the six 6×6 renormalization cells of the 216×72 simulation are used in a second simulation with a six-times coarser grid. The data from the 6×6 renormalization cell of this second simulation are then compared with the equivalent data from the 36×36 renormalization cell of the first simulation.

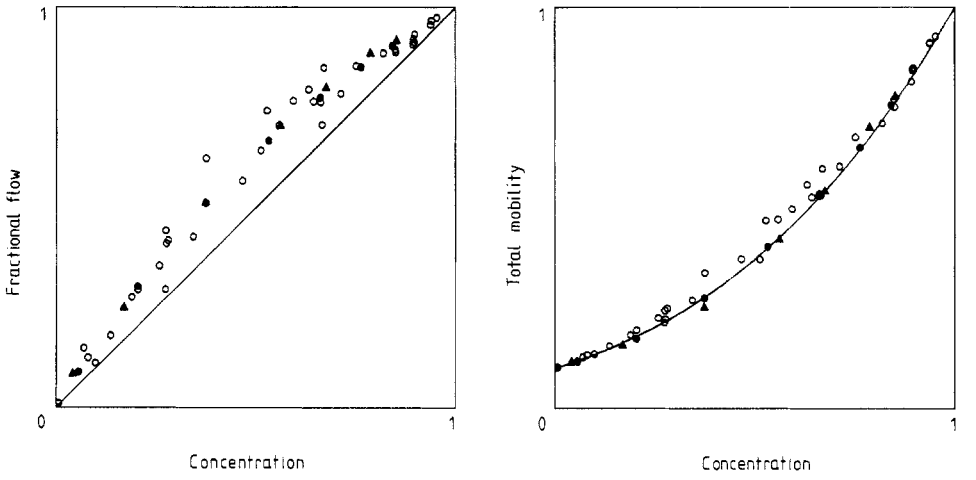

Figure 3. Fractional flow (*a*) and total mobility (*b*) data for the consistency test shown in figure 2: open circles for $[6\times6]$; filled circles for $[6\times6]^2$; filled triangles for $[36\times36]$.

mobility data at intermediate concentrations is characteristic of small values of the ratio w/m. The data in figure 1 suggest that boundary effects are seen for $w/m \leqslant 2$, but that they become unimportant for $w/m \geqslant 6$.

In addition we have found that provided that the above w/m criterion is satisfied, the proximity of the cell to the grid side boundary does not effect the data significantly: it is when the cell is simultaneously close to both side boundaries that boundary effects become seriously incorporated into the renormalized flow functions. For the larger two simulations mentioned above, the data shown in figure 1 were obtained from six cells placed across the drive. The advantage of using several cells in this manner is that several different fingering realizations are then represented in the data, thereby increasing the statistical significance of the results. The scatter present in the data from the two larger simulations is partly accounted for by this inclusion of several different realizations. However, we have also found that data from just one cell can be much more scattered if $w/m \geqslant 6$, than if $w/m \leqslant 2$.

We have tested this scheme as a true renormalization procedure as follows. The $[6\times6]$ flow functions computed from the 216×72 simulation shown in figure 1 were taken as grid block functions in a simulation using a grid six-times coarser, namely 36×12. From this simulation flow functions were computed corresponding to a cell of size 6×6 placed in the middle of the drive at 6–11 grid blocks inclusive. These data are then compared with those from a $[36\times36]$ renormalization of the original 216×72 simulation, using a cell placed in the middle of the drive at 32–67 grid blocks inclusive (see figure 2). The two sets of data are shown in figure 3, together with the data from the intermediate $[6\times6]$ renormalization and the original grid block functions. Both fractional flow and total mobility data for these two different renormalization routes are in very good agreement, showing that the routes are equivalent, as they should be, and that the renormalization technique is working consistently. A generic problem of numerical renormalization is the change in length scale associated with the numerical dispersion between renormalization levels. However, the closeness of agreement between the $[36\times36]$ data and the $[6\times6]^2$ data, which provides a measure of the accuracy of the procedure, suggests that numerical dispersion is not substantially affecting the results.

From figure 3 it can be seen that the fractional flow data for all three renormalizations are very similar, being somewhat increased over the original grid block function at intermediate concentrations. Again the total mobility data follow a different scenario. The data for the first $[6\times6]$ renormalization have increased at intermediate concentrations relative to the original grid block function, whereas the total mobility data from the larger renormalizations are hardly distinguishable from the original grid block functions. We believe that this change of behaviour in the total mobility data between the two renormalizations is due to the close proximity of the larger renormalization cell to the flow boundaries ($w/m=2$), as noted above. It appears that the inclusion of side boundary effects in the renormalized flow functions causes a reduction in the total mobility at intermediate concentrations, but has little effect on the fractional flow, as noted above in relation to the data in figure 1.

5. Results

Using the repeated renormalization technique described above, we have investigated the n–ω plane in the physically significant region ($|n| \leqslant 1, 0 \leqslant \omega \leqslant 1$) using a 108×36

grid to obtain renormalized data from six cells of size 6×6 placed at grid blocks 22–27 inclusive in the drive direction. In all cases where breakthrough significantly perturbed the flow, data after breakthrough were excluded from the computed renormalization. Data for two iterations starting from the point (0.25, 1.0) are shown in figure 4. For the first renormalization, both the fractional flow and the total mobility data are seen to increase at intermediate concentrations when compared with the grid block functions, though there is a significant amount of scatter in the data. This scatter limits the significance that can be attached to the fit to this data used in the second simulation. Of course a full statistical treatment would be more informative in this respect, but we restrict ourselves to considering only the mean behaviour. For the second renormalization, the increase at intermediate concentrations is rather less, and the data are much less scattered. (Note that regarding the total mobility data, this result is different from the case above where the second renormalization cell was strongly subject to boundary effects.) This behaviour can be best represented by motion in the n–ω plane, and the data from figure 4 are shown in this way in figure 5, together with our results.

The region of the n–ω plane shown in figure 5 appears to separate naturally into two parts roughly corresponding to whether ω is greater or less than approximately 0.55. For values of ω in the range $0.6 \leqslant \omega \leqslant 1.0$, the flow functions appear to converge under repeated renormalization to a point somewhere near (0.5, 0.6) in the n–ω plane. In principle further iterations could be made in an attempt to further isolate the exact nature of the motion in this region, but in practice it has to be borne in mind that the numerical renormalization procedure has only limited accuracy as indicated above, and that the degree of confidence represented by the data in figure 3 for the consistency test shown in figure 2 limits the progress that can be made in this way: because our simulation results contain a small but significant component of numerical dispersion, there is a danger that under repeated iteration of the renormalization, we stabilize the fingering through spurious finger suppressing dispersion terms. In general, including dispersion terms will drive the renormalization towards a lower value of ω than would otherwise be the case, since as ω decreases, the displacement tends to become more and more diffuse. Nonetheless, it is striking that the renormalizations from points on

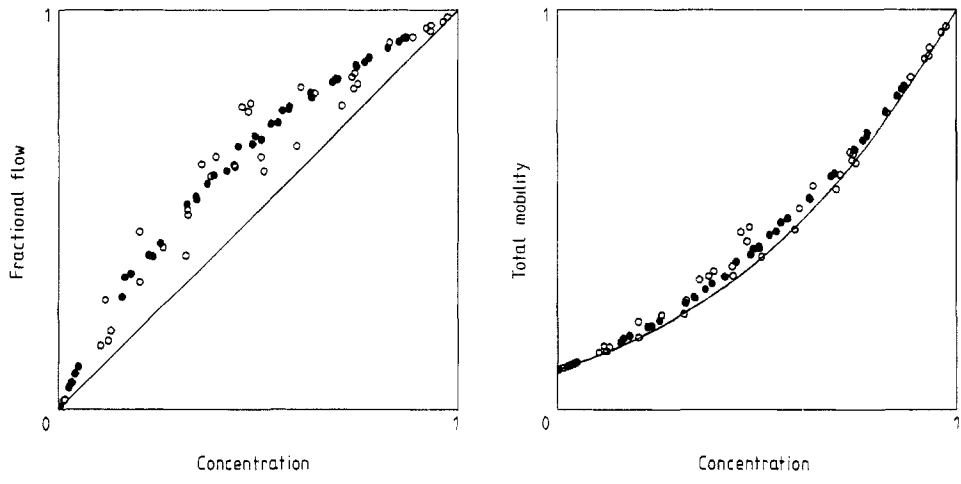

Figure 4. Fractional flow (*a*) and total mobility (*b*) data for $[6 \times 6]$ (open circles) and $[6 \times 6]^2$ (filled circles) renormalizations. The curves are the initial grid block functions.

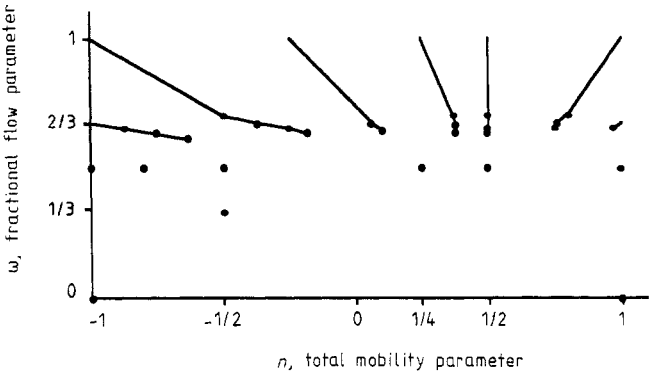

Figure 5. Effect of renormalization on the pseudo one-dimensional fractional flow and total mobility functions. Lines connect successive renormalizations from given initial values of n, ω. Isolated points represent initial values that do not change under renormalization, and generally correspond to flows in which fingering is substantially suppressed.

the line $\omega = 1.0$ have almost converged to the same fractional flow function after just two or three iterations—a linear scaling factor of approximately 100. Furthermore, due to the scatter in the data for the first renormalizations from these points, as exemplified in figure 4, it may be that this degree of convergence occurs still more quickly.

For values of ω in the range $0 \leqslant \omega \leqslant 0.5$, no motion has been observed under renormalization. Certainly for the points (0, 0) and (1.0, 0), the latter being the parallel flow case, the functions are immediately stationary, an effect associated with an absence of any significant fingering during the displacement, which of course forces the renormalized functions to take the grid block values. For these displacements the front is extremely diffuse. However, for the other points shown in this region, the fingering is less suppressed than in the $\omega = 0$ cases; it may be that motion in this area is much too slow to be measurable by our numerical scheme.

Although the data in figure 5 suggest that there is a substantial change of behaviour under renormalization approximately in the region of the line $\omega = 0.55$, as described above, this is not accompanied by a noticeable change in the fingering behaviour. Shown in figure 6 are contour plots of the concentration fields at $t = 0.25$ pore volumes for the points (0.5, 1.0), (0.5, 0.65) and (0.5, 0.5) in the n-ω plane. These plots show that as ω decreases, fingering is gradually suppressed, but no obvious evidence for transitional behaviour is observed.

We venture some interpretation of our results for the input of 'conventional' quarter power mixing rule miscible displacements. In this case the mobility rule, which is essentially an empirical account of experimental observation with fluid mixtures, is relatively stable under renormalization. By contrast the linear fractional flow function, $f(c) = c$, which comes from idealizing the mixture to be equivalent to a true single phase, changes significantly under renormalization, soon becoming an approximately stable function which appears to be universal for displacements exhibiting substantial fingering. The fingered mixture has a characteristic behaviour which is different from that of a truly mixed phase. This behaviour is most clearly represented in the fractional flow function, and is not very sensitive to the total mobility.

Is there a fixed point? Because of the reasons given above, this intriguing question is hard to address with confidence. Within the limitations of our results and their resolution, it appears that the fractional flow function converges under renormalization

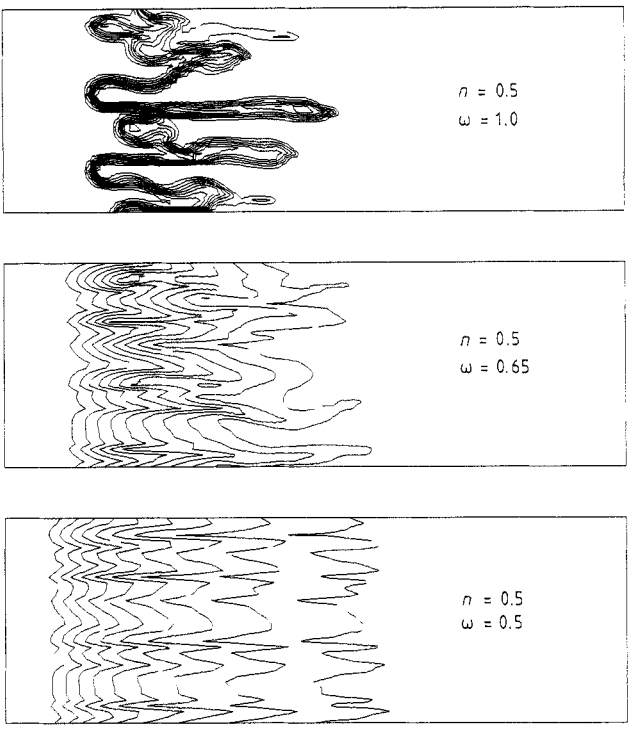

Figure 6. Contour plots of the concentration fields at $t = 0.25$ pore volumes for the points (0.5, 1.0), (0.5, 0.65) and (0.5, 0.5) in the n-ω plane. The contours are at intervals of 0.1, in the range 0.1 to 0.9. Injection is from left to right.

and for practical applications is effectively scale invariant beyond a linear scaling factor of about 100 units starting from 'conventional' quarter power displacements. Whether the total mobility function converges under renormalization is rather less clear. Consequently it is uncertain whether the observed behaviour is associated with a unique fixed point near (0.5, 0.6); another possibility is that not all renormalizations starting from the $\omega = 1.0$ line converge to the same point, and that there is a line of fixed points that marks the boundary of the apparently stationary region at approximately $\omega = 0.55$.

6. Conclusions

We have developed a self-consistent numerical renormalization scheme for prescribing miscible flow functions for use in reservoir scale simulations, given core scale flow data. Using this scheme we have found that the fractional flow function becomes scale invariant for practical purposes beyond a linear scaling factor of approximately 100, and that the invariant function appears to be universal for displacements exhibiting substantial fingering. The effect of renormalization on the total mobility function is less well established. Consequently, it is not clear whether there is a unique fixed point to which all displacements exhibiting substantial fingering eventually converge under renormalization, or whether, in the absence of such convergence, there is a line of

fixed points. The size of real reservoirs corresponds, in our scheme, to only approximately four renormalizations from the core scale (plus the final simulation). As a result, we can confidently predict that the total mobility does not converge to a universal function in practise.

All the work presented here is concerned with miscible flooding in homogeneous systems at a viscosity ratio of 10. We intend to extend this work to other viscosity ratios, to discover the effect of this parameter on the structure of figure 5. Another area for development is the matter of heterogeneous permeabilities, which is of considerable importance in the context of realistic models for reservoir systems.

Acknowledgments

We would like to thank the British Petroleum Company plc for supporting this work, and giving permission to publish these results. We would particularly like to thank Dr M Christie for the use of his simulation code, and Dr P King for many helpful discussions.

References

Christie M A 1988 Application of high resolution simulation to modelling fluid instabilities *Mathematics in Oil Production* ed S F Edwards and P R King (Oxford: Clarendon) pp 269-84

Christie M A and Bond D J 1987 *Soc. Pet. Eng. Reservoir Eng.* **2** 514-22

Koval E J 1963 *SPEJ Trans. AIME* **228** 145-54

Scheidegger A E 1971 *The Physics of Flow Through Porous Media* Section 9.4 (Toronto: University of Toronto) pp 229-38

Todd M R and Longstaff W J 1972 *JPT Trans. AIME* **253** 874-82